Eur. Phys. J. C 27, 87–99 (2003)
Digital Object Identifier (DOI) 10.1140/epjc/s2002-01106-2

THE EUROPEAN PHYSICAL JOURNAL C

J/ψ production at HERA in the color singlet model with $k_{\rm T}$-factorization

A.V. Lipatov[1,a], N.P. Zotov[2,b]

[1] Physical Department, M.V. Lomonosov Moscow State University, 119992 Moscow, Russia
[2] D.V. Skobeltsyn Institute of Nuclear Physics, M.V. Lomonosov Moscow State University, 119992 Moscow, Russia

Received: 31 October 2002 /
Published online: 24 January 2003 –

Abstract. In the framework of the $k_{\rm T}$-factorization QCD approach and the color singlet model we consider J/ψ inelastic photo- and leptoproduction processes at HERA. We investigate the dependences of the single differential and double differential cross section on various forms of the unintegrated gluon distribution. The z and $\mathbf{p}_{\rm T}$ dependences of the spin alignment parameter α are presented also. Our theoretical predictions agree well with the recent data taken by the H1 and ZEUS collaborations at HERA. It is shown that the experimental study of the polarization J/ψ mesons at the low value $Q^2 < 1\,{\rm GeV}^2$ is an additional test of BFKL gluon dynamics.

1 Introduction

It is known that from heavy quark and quarkonium production processes one can obtain unique information on the gluon structure function of the proton because of the dominance of the photon–gluon or gluon–gluon fusion subprocess in the framework of QCD [1]. Studying gluon distributions at a modern collider energy (such as HERA, Tevatron) is important for the prediction of heavy quark and quarkonium production cross sections at future colliders (LHC, THERA). At the energies of the HERA and LEP/LHC colliders heavy quark and quarkonium production processes are so-called semihard processes [2–5]. In such processes by definition the hard scattering scale $\mu \sim m_Q$ is large compared to the $\Lambda_{\rm QCD}$ parameter, but on the other hand μ is much less than the total center-of-mass energy: $\Lambda_{\rm QCD} \ll \mu \ll s^{1/2}$. The latter condition implies that the processes occur in the small x region: $x \simeq m_Q/s^{1/2} \ll 1$, and that the cross sections of heavy quark and quarkonium production processes are determined by the behavior of the gluon distributions in the small x region.

It is also known that in the small x region the standard parton model (SPM) assumptions about factorization of the gluon distribution functions and subprocess cross sections are broken because the subprocess cross sections and gluon structure functions depend on the gluon transverse momentum $k_{\rm T}$ [2–5]. Thus calculations of heavy quark production cross sections at the HERA, Tevatron, LHC and other collider conditions are necessarily carried out in the so-called $k_{\rm T}$-factorization (or semihard) QCD approach, which is more preferable for the small x region than SPM.

The $k_{\rm T}$-factorization QCD approach is based on the Balitsky, Fadin, Kuraev, Lipatov (BFKL) [6] evolution equations. The resummation of the terms $\alpha_{\rm S}^n \ln^n(\mu^2/\Lambda^2_{\rm QCD})$, $\alpha_{\rm S}^n \ln^n(\mu^2/\Lambda^2_{\rm QCD}) \ln^n(1/x)$ and $\alpha_{\rm S}^n \ln^n(1/x)$ in the $k_{\rm T}$-factorization approach leads to the unintegrated (dependent on $\mathbf{q}_{\rm T}$) gluon distribution $\Phi(x, \mathbf{q}_{\rm T}^2, \mu^2)$ which determines the probability to find a gluon carrying the longitudinal momentum fraction x and the transverse momentum $\mathbf{q}_{\rm T}$ at the probing scale μ^2.

To calculate the cross section of a physical process the unintegrated gluon distributions have to be convoluted with off mass shell matrix elements corresponding to the relevant partonic subprocesses [2–5]. In the off mass shell matrix element the virtual gluon polarization tensor is taken in the BFKL form [2–5]

$$L^{\mu\nu}(q) = \frac{q_{\rm T}^\mu q_{\rm T}^\nu}{\mathbf{q}_{\rm T}^2}. \qquad (1)$$

Nowadays, the significance of the $k_{\rm T}$-factorization QCD approach becomes more and more commonly recognized [7]. It was already used for the description of a wide class heavy quark and quarkonium production processes [8–23]. It is notable that calculations in the $k_{\rm T}$-factorization approach provide results which are absent in other approaches, such as the fast growth of the total cross sections in comparison with SPM, a broadening of the $p_{\rm T}$ spectra due to the extra transverse momentum of the colliding partons and other polarization properties of the final particles in comparison with SPM.

We point out that heavy quark and quarkonium cross section calculations within the SPM in fixed order pQCD

[a] e-mail: artem_lipatov@mail.ru
[b] e-mail: zotov@theory.sinp.msu.ru

have some problems. For example, a very large discrepancy (by more than an order of magnitude) [24,25] between the pQCD predictions for hadroproduction J/ψ and Υ mesons and experimental data at Tevatron was found. This fact has resulted in intensive theoretical investigations of such processes. In particular, it was required to use an additional transition mechanism from the $c\bar{c}$-pair to the J/ψ mesons, the so-called the color octet (CO) model [26], where a $c\bar{c}$-pair is produced in the color octet state and transforms into a final color singlet (CS) state by the help of soft gluon radiation. The CO model was supposed to be applicable to heavy quarkonium hadro- and leptoproduction processes. However, the contributions from the CO mechanism to the J/ψ meson photoproduction contradict the experimental data at HERA for the z distribution [27–30].

Another difficulty of the CO model is the J/ψ polarization properties in $p\bar{p}$-interactions at the Tevatron. In the framework of the CO model, the J/ψ mesons should be transversally polarized at large transverse momenta $\mathbf{p}_{\rm T}$. However, this is in contradiction with the experimental data, too.

The CO model has been applied earlier [31,32] in an analysis of the J/ψ inelastic production experimental data at HERA [33]. However, the results do not agree with each other [32]. We note that the shapes of the Q^2, $\mathbf{p}_{\rm T}^2$ and y^* distributions are not reproduced by the calculation [31], and the z distributions [32] contradict the HERA experimental data too. Results obtained within the usual collinear approach and CS model [34–37] underestimate the experimental data by about a factor 2.

The inelastic J/ψ production at HERA in the CS model with $k_{\rm T}$-factorization also was considered in [15,16]. The results [16] agree with the H1 experimental data [33] both in normalization and shape only at a quite small charmed quark mass $m_c = 1.4\,\text{GeV}$. The theoretical predictions [15] have simulated the experimental analysis of the J/ψ polarization properties at HERA conditions.

Recently new experimental data on the inelastic J/ψ photo- and leptoproduction at HERA were obtained by the H1 [38,39] and ZEUS [40] collaborations with increased statistics and precision as compared with previous experimental analyses [33]. Based on the above mentioned results here we will use the CS model and the $k_{\rm T}$-factorization approach for the analysis of the data [38–40]. We investigate the dependences of the single differential and double differential J/ψ production cross section on various forms of the unintegrated gluon distribution. Special attention is drawn to the unintegrated gluon distributions obtained from the BFKL evolution equation which has been applied earlier in our previous papers [12–16]. For studying the J/ψ meson polarization properties we calculate the z and $\mathbf{p}_{\rm T}$ dependences of the spin alignment parameter α.

The outline of this paper is as follows. In Sect. 2 we present, in analytic form, the total and differential cross section for the inelastic J/ψ photo- and leptoproduction in the CS model with $k_{\rm T}$-factorization, and give the formulas for the relevant partonic subprocess off mass shell matrix elements. In Sect. 3 we present the numerical results of our calculations and compare them with the H1 [38,39] and ZEUS [40] data. Finally, in Sect. 4, we give some conclusions.

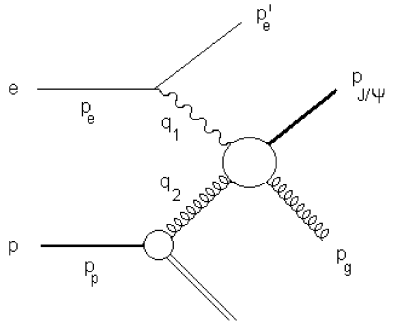

Fig. 1. Diagram for $ep \to e' J/\psi X$ process

2 Analytic results

In this section we calculate the total and differential cross section for inelastic J/ψ photo- and leptoproduction in the CS model with $k_{\rm T}$-factorization, and give the formulas for the relevant partonic subprocess off mass shell matrix elements.

2.1 Kinematics

As indicated in Fig. 1, we denote the 4-momenta of the incoming electron and proton and the outgoing electron, proton remnant, J/ψ meson and gluon by p_e, p_p, p'_e, p'_p, p_ψ and p_g, respectively. The initial virtual photon and BFKL gluon have 4-momenta $q_1 = p_e - p'_e$ and $q_2 = p_p - p'_p$, so that the 4-momentum transfer $Q^2 = -q_1^2$. In our analysis below we will use the Sudakov decomposition, which has the following form:

$$p_\psi = \alpha_1 p_e + \beta_1 p_p + p_{\psi\rm T}, \quad p_g = \alpha_2 p_e + \beta_2 p_p + p_{g\rm T},$$
$$q_1 = x_1 p_e + q_{1\rm T}, \quad q_2 = x_2 p_p + q_{2\rm T}, \tag{2}$$

where $p_{\psi\rm T}$, $p_{g\rm T}$, $q_{1\rm T}$ and $q_{2\rm T}$ are the transverse 4-momenta of the corresponding particles, and

$$p_\psi^2 = m_\psi^2, \quad p_g^2 = 0, \quad q_1^2 = q_{1\rm T}^2, \quad q_2^2 = q_{2\rm T}^2. \tag{3}$$

In the ep c.m. frame we can write

$$p_e = \sqrt{s}/2(1,0,0,1), \quad p_p = \sqrt{s}/2(1,0,0,-1), \tag{4}$$

where we neglect the masses of the electron and proton. The Sudakov variables are expressed as follows:

$$\alpha_1 = \frac{m_{\psi\rm T}}{\sqrt{s}}\exp(y_\psi), \quad \alpha_2 = \frac{|\mathbf{p}_{g\rm T}|}{\sqrt{s}}\exp(y_g),$$
$$\beta_1 = \frac{m_{\psi\rm T}}{\sqrt{s}}\exp(-y_\psi), \quad \beta_2 = \frac{|\mathbf{p}_{g\rm T}|}{\sqrt{s}}\exp(-y_g), \tag{5}$$

where $m^2_{\psi\rm T} = m^2_\psi + \mathbf{p}^2_{\psi\rm T}$, y_ψ and y_g are the rapidities of J/ψ meson and final gluon respectively in the ep c.m. frame. From the conservation laws we can easily obtain the following conditions:

$$x_1 = \alpha_1 + \alpha_2, \quad x_2 = \beta_1 + \beta_2, \quad \mathbf{q}_{1\rm T} + \mathbf{q}_{2\rm T} = \mathbf{p}_{\psi\rm T} + \mathbf{p}_{g\rm T}. \tag{6}$$

Also the variable $z = (p_\psi \cdot p_p)/(q_1 \cdot p_p)$ is used for a description of the quarkonium photo- and leptoproduction processes. In the rest frame of the proton one has $z = E_\psi/E_\gamma$.

2.2 Inelastic J/ψ leptoproduction cross section

In the $k_{\rm T}$-factorization approach the differential cross section for inelastic J/ψ leptoproduction may be written as

$$\begin{aligned}&{\rm d}\sigma(ep \to e' J/\psi X) \\ &= \frac{{\rm d}x_2}{x_2} \Phi(x_2, \mathbf{q}^2_{2\rm T}, \mu^2) \frac{{\rm d}\phi_2}{2\pi} {\rm d}\mathbf{q}^2_{2\rm T} {\rm d}\hat{\sigma}(eg^* \to e' J/\psi g'),\end{aligned} \tag{7}$$

where ϕ_2 is the initial BFKL gluon azimuthal angle, and $\Phi(x_2, \mathbf{q}^2_{2\rm T}, \mu^2)$ is the unintegrated gluon distribution in the proton. The $eg^* \to e' J/\psi g'$ cross section is given by

$$\begin{aligned}&{\rm d}\hat{\sigma}(eg^* \to e' J/\psi g') \\ &= \frac{(2\pi)^4}{2x_2 s} \sum |M|^2_{\rm SHA}(eg^* \to e' J/\psi g') \\ &\times \frac{{\rm d}^3 p'_e}{(2\pi)^3 2p'^0_e} \frac{{\rm d}^3 p_\psi}{(2\pi)^3 2p^0_\psi} \frac{{\rm d}^3 p_g}{(2\pi)^3 2p^0_g} \\ &\times \delta^{(4)}(p_e + q_2 - p'_e - p_\psi - p_g),\end{aligned} \tag{8}$$

where $\sum |M|^2_{\rm SHA}(eg^* \to e' J/\psi g')$ is the off mass shell matrix element. In (8) $\sum$ indicates an averaging over and a sum over the final polarization states. From (7) and (8) we obtain the following formula for the inelastic J/ψ leptoproduction differential cross section in the $k_{\rm T}$-factorization approach:

$$\begin{aligned}&{\rm d}\sigma(ep \to e' J/\psi X) \\ &= \frac{1}{128\pi^3} \frac{\Phi(x_2, \mathbf{q}^2_{2\rm T}, \mu^2)}{(x_2 s)^2 (1 - x_1)} \frac{{\rm d}z}{z(1-z)} {\rm d}y_\psi \\ &\times \sum |M|^2_{\rm SHA}(eg^* \to e' J/\psi g') {\rm d}\mathbf{p}^2_{\psi\rm T} {\rm d}Q^2 {\rm d}\mathbf{q}^2_{2\rm T} \\ &\times \frac{{\rm d}\phi_1}{2\pi} \frac{{\rm d}\phi_2}{2\pi} \frac{{\rm d}\phi_\psi}{2\pi},\end{aligned} \tag{9}$$

where ϕ_1 and ϕ_ψ are the azimuthal angles of the initial virtual photon and J/ψ meson respectively.

2.3 Inelastic J/ψ photoproduction cross section

As in the leptoproduction case, in the $k_{\rm T}$-factorization approach the differential cross section for inelastic J/ψ photoproduction may be written as

$$\begin{aligned}&{\rm d}\sigma(\gamma p \to J/\psi X) \\ &= \frac{{\rm d}x_2}{x_2} \Phi(x_2, \mathbf{q}^2_{2\rm T}, \mu^2) \frac{{\rm d}\phi_2}{2\pi} {\rm d}\mathbf{q}^2_{2\rm T} {\rm d}\hat{\sigma}(\gamma g^* \to J/\psi g').\end{aligned} \tag{10}$$

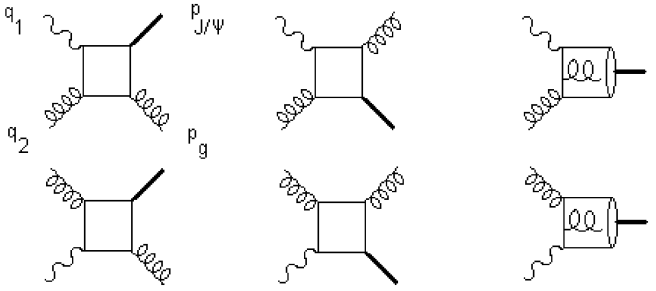

Fig. 2. Feynman diagram used for the description of the partonic $\gamma g \to J/\psi g'$ process

If we take the limit $Q^2 \to 0$ and $x_1 \to 1$, we easy obtain the following formula for the inelastic J/ψ photoproduction differential cross section in the $k_{\rm T}$-factorization approach by analogy with the leptoproduction case:

$$\begin{aligned}&{\rm d}\sigma(\gamma p \to J/\psi X) \\ &= \frac{1}{16\pi (x_2 s)^2} \Phi(x_2, \mathbf{q}^2_{2\rm T}, \mu^2) \frac{{\rm d}z}{z(1-z)} \\ &\times \sum |M|^2_{\rm SHA}(\gamma g^* \to J/\psi g') {\rm d}\mathbf{p}^2_{\psi\rm T} {\rm d}\mathbf{q}^2_{2\rm T} \frac{{\rm d}\phi_2}{2\pi} \frac{{\rm d}\phi_\psi}{2\pi}.\end{aligned} \tag{11}$$

We note that formulas for the differential cross section for inelastic J/ψ photo- and leptoproduction in the usual parton model may be obtained from (9) and (11), if we take the limit $\mathbf{q}^2_{2\rm T} \to 0$ and average them over the transverse momentum vector $\mathbf{q}_{2\rm T}$.

2.4 Off mass shell matrix element

There are six Feynman diagrams (Fig. 2) which describe the partonic subprocess $\gamma g^* \to J/\psi g'$ at leading order in $\alpha_{\rm S}$ and α. In the framework of the CS model and the non-relativistic approximation the production of the J/ψ meson is considered as production of a quark–antiquark system in the color singlet state with orbital momentum $L = 0$ and spin momentum $S = 1$. The binding energy and relative momentum of the quarks in the J/ψ meson are neglected, resulting in $m_\psi = 2m_c$, where m_c is the charm mass. The amplitude of the process $\gamma g^* \to J/\psi g'$ may be obtained from the amplitude of the process $\gamma g^* \to c\bar{c} g'$ after the replacement

$$v(p_{\bar{c}}) \bar{u}(p_c) \to \hat{J}(p_\psi) = \frac{\psi(0)}{2\sqrt{m_\psi}} \hat{\epsilon}(p_\psi)(\hat{p}_\psi + m_\psi) \frac{1}{\sqrt{3}}, \tag{12}$$

where $p_c = p_\psi/2$, $\epsilon(p_\psi)$ is the 4-vector of the J/ψ polarization, $1/(3^{1/2})$ is the color factor, and $\psi(0)$ is the non-relativistic meson wave function at the origin. The matrix element is

$$\begin{aligned}M &= e_c g^2 \epsilon_\mu(q_1) \epsilon_\sigma(q_2) \epsilon_\rho(p_g) \\ &\times {\rm Sp}\left[\hat{J}(p_\psi) \gamma^\mu \frac{\hat{p}_c - \hat{q}_1 + m_c}{(p_c - q_1)^2 - m_c^2} \gamma^\sigma \frac{-\hat{p}_c - \hat{p}_g + m_c}{(-p_c - p_g)^2 - m_c^2} \gamma^\rho\right]\end{aligned} \tag{13}$$

+ 5 permutations of all gauge bosons. Here $\epsilon_\mu(q_1)$ and $\epsilon_\mu(q_2)$ are polarization vectors of the initial photon and

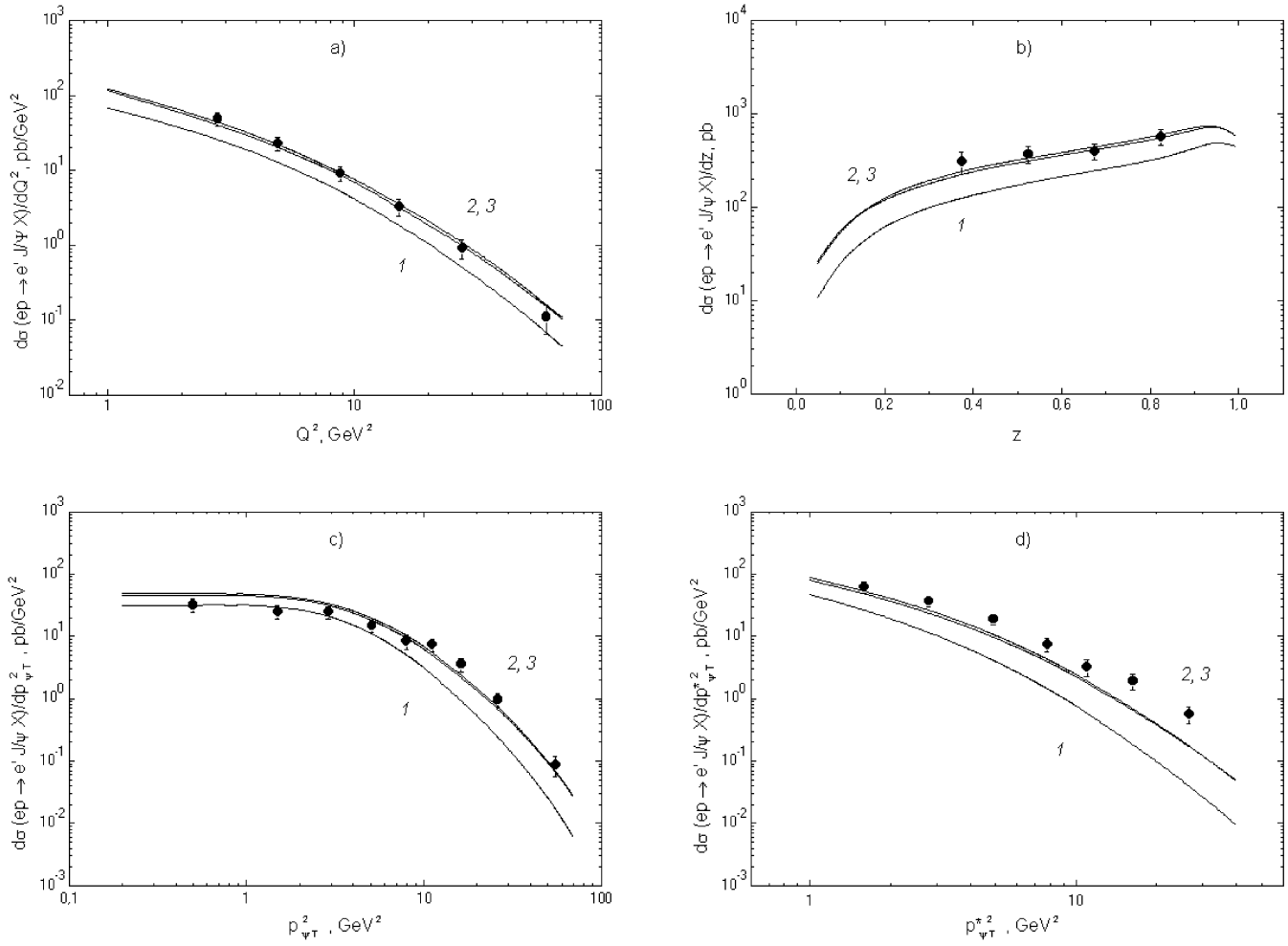

Fig. 3a–g. The single differential cross sections of the inelastic J/ψ leptoproduction obtained in the kinematical region $2 < Q^2 < 100\,\mathrm{GeV}^2$, $50 < W < 225\,\mathrm{GeV}$, $0.3 < z < 0.9$ and $p^{*2}_{\psi\mathrm{T}} > 1\,\mathrm{GeV}^2$ at $s^{1/2} = 314\,\mathrm{GeV}$ in comparison with the H1 [39] data. Curve 1 corresponds to the SPM calculations at the leading order approximation with GRV (LO) gluon density, curves 2 and 3 correspond to the $k_{\rm T}$-factorization QCD calculations with the JB and KMS unintegrated gluon distribution

gluon respectively, $\epsilon_\mu(p_g)$ is the 4-vector of the final gluon polarization. The summation on the J/ψ meson and final gluon polarizations is carried out by the covariant formulas

$$\sum \epsilon^\mu(p_\psi)\epsilon^{*\nu}(p_\psi) = -g^{\mu\nu} + \frac{p^\mu_\psi p^\nu_\psi}{m^2_\psi}, \qquad (14)$$

$$\sum \epsilon^\mu(p_g)\epsilon^{*\nu}(p_g) = -g^{\mu\nu}. \qquad (15)$$

The initial BFKL gluon polarization tensor is taken in the form (1). For the photon we use the usual expression:

$$\sum \epsilon^\mu(q_1)\epsilon^{*\nu}(q_1) = -g^{\mu\nu} \qquad (16)$$

in the photoproduction case and the full lepton tensor (including also the photon propagator factor and photon–lepton coupling) in the leptoproduction case:

$$\sum \epsilon^\mu(q_1)\epsilon^{*\nu}(q_1) = 2\frac{e^2}{Q^2}\left(-g^{\mu\nu} + \frac{4p^\mu_e p^\nu_e}{Q^2}\right). \qquad (17)$$

For studying J/ψ polarized production we introduce the 4-vector of the longitudinal polarization $\epsilon^\mu_{\rm L}(p_\psi)$ as follows [41]:

$$\epsilon^\mu_{\rm L}(p_\psi) = \frac{(p_\psi \cdot p_p)}{\sqrt{(p_\psi \cdot p_p)^2 - m^2_\psi s}}\left(\frac{p^\mu_\psi}{m_\psi} - \frac{m_\psi p^\nu_p}{(p_\psi \cdot p_p)}\right). \qquad (18)$$

The evaluation of $\sum |M|^2_{\rm SHA}$ for the photo- and leptoproduction cases was done analytically by the REDUCE program. Also in our calculations we have used the JB [42] and KMS [43] parameterizations of the unintegrated gluon distributions (see also [7] for information on details).

3 Numerical results

In this section we present the theoretical results in comparison with recent experimental data taken by the H1 [38,39] and ZEUS [40] collaborations at HERA.

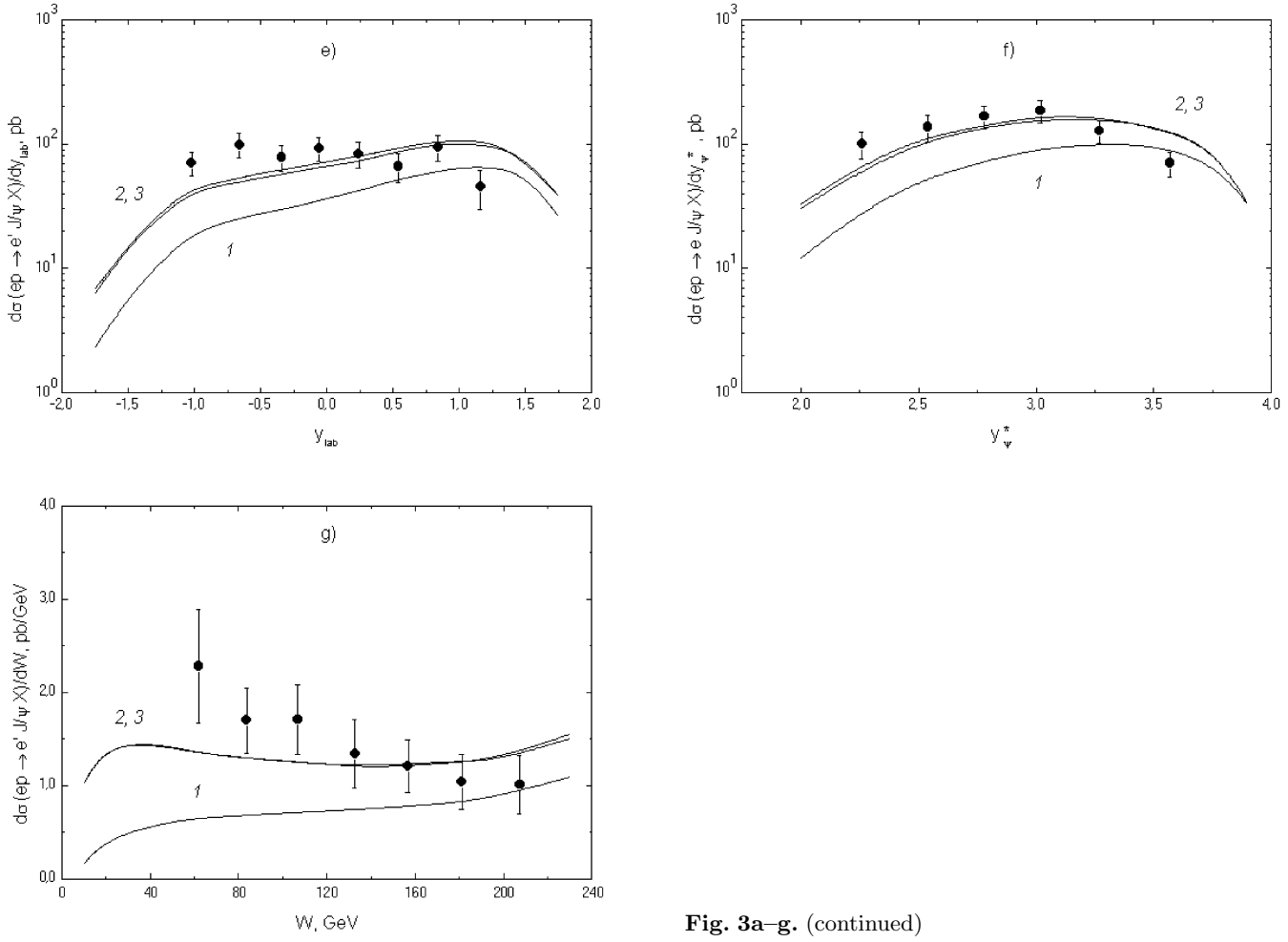

Fig. 3a–g. (continued)

There are three parameters which determine the common normalization factor of the cross section under consideration: the J/ψ meson wave function at the origin $\psi(0)$, the charmed quark mass m_c and factorization scale μ. The value of the J/ψ meson wave function at the origin may be calculated in a potential model or obtained from the well-known experimental decay width $\Gamma(J/\psi \to \mu^+\mu^-)$. In our calculation we used $|\psi(0)|^2 = 0.0876\,\mathrm{GeV}^3$ as in [44].

Concerning the charmed quark mass, the situation is not clear: on the one hand, in the non-relativistic approximation one has $m_c = m_\psi/2 = 1.55\,\mathrm{GeV}$, but on the other hand there are examples when a smaller value of the charm mass, $m_c = 1.4\,\mathrm{GeV}$, is used [32,45]. However, in our previous paper [16] we analyzed in detail the influence of the charm quark mass on the theoretical results. We found that the main effect of a change of the charm quark mass connects with the final phase space of the J/ψ meson, and in the subprocess matrix elements this effect is negligible. Taking into account that the value of $m_c = 1.4\,\mathrm{GeV}$ corresponds to the unphysical phase space of the J/ψ state, in the present paper we will use the value of the charm mass $m_c = 1.55\,\mathrm{GeV}$ only.

Also the most significant theoretical uncertanties come from the choice of the factorization scale $\mu_{\rm F}$ and the renormalization one $\mu_{\rm R}$. One of them is related to the evolution of the gluon distributions $\Phi(x, \mathbf{q}_{\rm T}^2, \mu_{\rm F}^2)$, the other is responsible for the strong coupling constant $\alpha_{\rm S}(\mu_{\rm R}^2)$. As often done in the literature, we set $\mu_{\rm F} = \mu_{\rm R} = \mu$. In the present paper we used the following choice $\mu^2 = \mathbf{q}_{2\rm T}^2$ as in [16,46].

3.1 Inelastic J/ψ leptoproduction at HERA

The integration limits in (9) are taken as given by kinematical conditions of the H1 experimental data [39]. One kinematical region[1] is $2 < Q^2 < 100\,\mathrm{GeV}^2$, $50 < W < 225\,\mathrm{GeV}$, $0.3 < z < 0.9$, $\mathbf{p}^{*2}_{\psi\rm T} > 1\,\mathrm{GeV}^2$ and the other kinematical region is $12 < Q^2 < 100\,\mathrm{GeV}^2$, $50 < W < 180\,\mathrm{GeV}$, $\mathbf{p}^2_{\psi\rm T} > 6.4\,\mathrm{GeV}^2$, $0.3 < z < 0.9$ and $\mathbf{p}^{*2}_{\psi\rm T} > 1\,\mathrm{GeV}^2$. Here and in the following, we used $\Lambda_{\rm QCD} = 250\,\mathrm{MeV}$.

The results of our calculations are shown in Figs. 3–5. Figure 3 shows the single differential cross sections of the inelastic J/ψ meson leptoproduction obtained in the

[1] Here we denote the J/ψ meson transverse momentum and rapidity in the $\gamma^* p$ c.m. frame by $\mathbf{p}^*_{\psi\rm T}$ and y^*_ψ, respectively

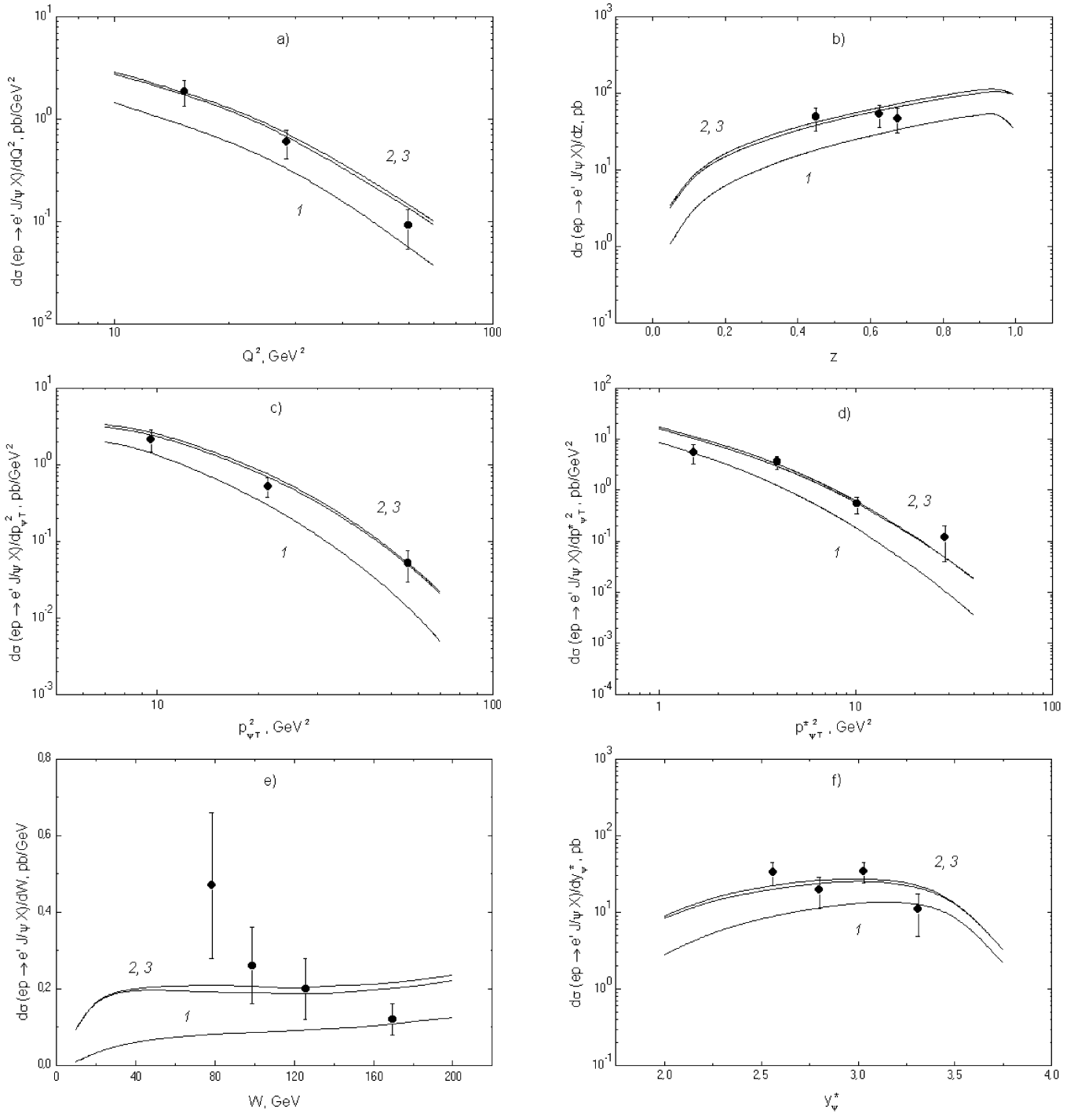

Fig. 4a–f. The single differential cross sections of the inelastic J/ψ leptoproduction obtained in the kinematical region $12 < Q^2 < 100\,\mathrm{GeV}^2$, $50 < W < 225\,\mathrm{GeV}$, $p^2_{\psi\mathrm{T}} > 6.4\,\mathrm{GeV}^2$, $0.3 < z < 0.9$ and $p^{*2}_{\psi\mathrm{T}} > 1\,\mathrm{GeV}^2$ at $s^{1/2} = 314\,\mathrm{GeV}$ in comparison with the H1 [39] data. Curves 1–3 are the same as in Fig. 3

first kinematical region at $s^{1/2} = 314\,\mathrm{GeV}$. Curve 1 corresponds to the SPM calculations at the leading order approximation with the GRV (LO) gluon density, curves 2 and 3 correspond to the $k_{\rm T}$-factorization results with the JB (at $\Delta = 0.35$ [17,23]) and the KMS unintegrated gluon distributions. One can see that the results obtained in the CS model with $k_{\rm T}$-factorization agree very well with the H1 experimental data. The SPM calculations are lower than the data by a factor 2–3.

We would like to note the difference in the transverse momenta distribution shapes between the curves obtained using the $k_{\rm T}$-factorization approach and the SPM. This difference is manifest in the $p_{\rm T}$ broadening effect which was mentioned before. It is visible also that only the $k_{\rm T}$-

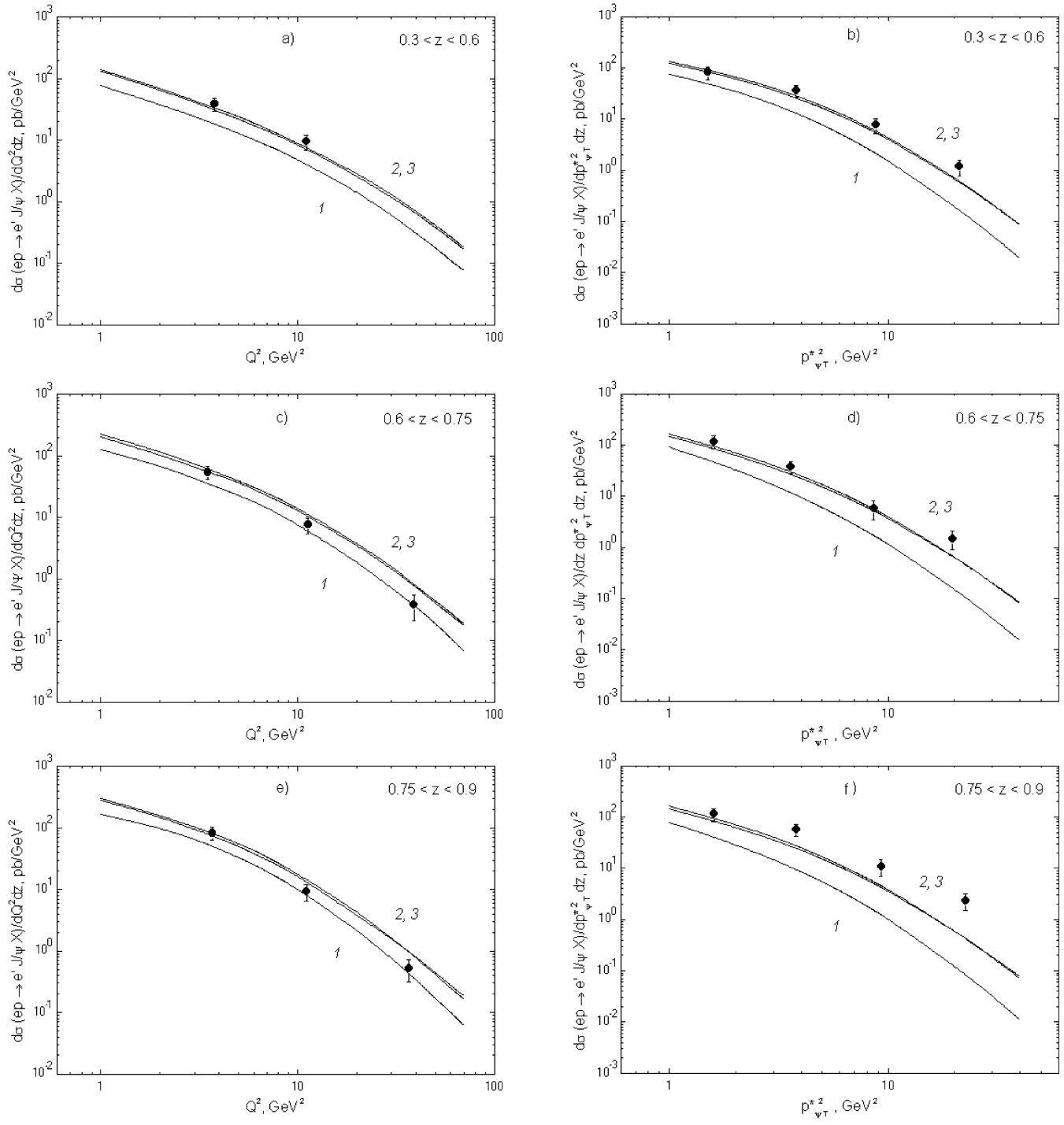

Fig. 5a–f. The double differential cross sections of the inelastic J/ψ leptoproduction obtained in the kinematical region $2 < Q^2 < 100\,\mathrm{GeV}^2$, $50 < W < 225\,\mathrm{GeV}$, $0.3 < z < 0.9$ and $p^{*2}_{\psi\mathrm{T}} > 1\,\mathrm{GeV}^2$ at $s^{1/2} = 314\,\mathrm{GeV}$ in comparison with the H1 [39] data. Curves 1–3 are the same as in Fig. 3

factorization approach gives a correct description of the $\mathbf{p}^2_{\psi\mathrm{T}}$ spectra. However, we note that the $\mathbf{p}^{*2}_{\psi\mathrm{T}}$ distributions are somewhat less well described (in contrast with the $\mathbf{p}^2_{\psi\mathrm{T}}$ spectra) at large values of the J/ψ transverse momenta (see Fig. 3d).

Also we point out the good description of the z distributions which obtained in the $k_{\rm T}$-factorization approach in contrast with CO model results [32], except for the region $z < 0.3$, where the contribution of the resolved photon process may be large [47].

Figure 4 shows the single differential cross sections of the inelastic J/ψ meson production obtained in the second kinematical region at $s^{1/2} = 314\,\mathrm{GeV}$. Curves 1–3 are the same as in Fig. 3. We find also good agreement

between the results obtained in the CS model with $k_{\rm T}$-factorization and the H1 data. It is notable that in this kinematical region in contrast with the first one both $\mathbf{p}^2_{\psi\rm T}$ and $\mathbf{p}^{*2}_{\psi\rm T}$ transverse momenta distributions agree well with the experimental data.

The double differential cross sections $\mathrm{d}\sigma/\mathrm{d}Q^2\mathrm{d}z$ and $\mathrm{d}\sigma/\mathrm{d}\mathbf{p}^{*2}_{\psi\rm T}\mathrm{d}z$ (Fig. 5) obtained with $k_{\rm T}$-factorization in the different z regions $0.3 < z < 0.6$ (Fig. 5a,b), $0.6 < z < 0.75$ (Fig. 5c,d) and $0.75 < z < 0.9$ (Fig. 5e,f) agree with the H1 data. We note that the double differential cross sections $\mathrm{d}\sigma/\mathrm{d}\mathbf{p}^{*2}_{\psi\rm T}\mathrm{d}z$ are somewhat less well described at large z (see Fig. 5f). However, in this region the contribution of the diffractive processes may be large. None of these contributions are in our consideration.

It is interesting to note that results obtained with the JB unintegrated gluon distribution at $\Delta = 0.35$ and the KMS ones, which effectively included about 70% of the full NLO corrections to the value of Δ [43], coincide practically in a wide kinematical region.

Figures 3–5 show that the $k_{\rm T}$-factorization results for inelastic J/ψ leptoproduction with the realistic value of the charm mass of $m_c = 1.55\,\mathrm{GeV}$ agree well with the H1 experimental data without any additional $c\bar{c} \to J/\psi$ fragmentation mechanisms, such as the CO contributions.

3.2 Inelastic J/ψ photoproduction at HERA

The integration limits in (11) are taken as given by the kinematical conditions of the H1 [38] and the ZEUS [40] data. One kinematical region which corresponds to the H1 experiment is $60 < W < 240\,\mathrm{GeV}$, $0.3 < z < 0.9$, $1 < \mathbf{p}^2_{\psi\rm T} < 60\,\mathrm{GeV}^2$ and the other kinematical region which corresponds to the ZEUS experiment is $50 < W < 180\,\mathrm{GeV}$, $0.4 < z < 0.9$, $\mathbf{p}^2_{\psi\rm T} > 1\,\mathrm{GeV}^2$.

The results of our calculations are shown in Figs. 6–8. Figures 6 and 7 show the total and single differential cross sections of inelastic J/ψ meson photoproduction in comparison with the H1 and ZEUS data, respectively. As in the previous section, curve 1 corresponds to the SPM calculations at the leading order approximation with the GRV (LO) gluon density, curves 2 and 3 correspond to the $k_{\rm T}$-factorization results with the JB (at $\Delta = 0.35$ [17,23]) and KMS unintegrated gluon distributions.

The W dependences of the total J/ψ photoproduction cross section at $0.3 < z < 0.9$, $0.3 < z < 0.8$ and $0.4 < z < 0.9$ are plotted in Figs. 6a,b and 7a respectively. One can see that results obtained in the CS model with $k_{\rm T}$-factorization agree very well with the H1 [38] and the ZEUS [40] experimental data. The SPM results are lower than the data by a factor of 2.

Concerning the shapes of the $\mathbf{p}^2_{\psi\rm T}$ distribution (Figs. 6c and 7b), one can note a difference between the $k_{\rm T}$-factorization and the SPM curves. As in the leptoproduction case, this difference is manifest in the $p_{\rm T}$ broadening effect which was mentioned earlier. It is visible also that only the $k_{\rm T}$-factorization approach gives a correct description of the H1 and ZEUS data.

The z distributions are shown in Figs. 6d,e,f and 7c,d,e at different $\mathbf{p}_{\psi\rm T}$ cuts in comparison with the H1 and ZEUS data, respectively. Good agreement between the $k_{\rm T}$-factorization curves and the experimental data is observed. The z distribution are somewhat less well described at $\mathbf{p}_{\psi\rm T} > 3\,\mathrm{GeV}$ (see Fig. 6f). The discrepancy between the leading order SPM calculations and the experimental data is about a factor of 2 at $\mathbf{p}_{\psi\rm T} > 1\,\mathrm{GeV}$ and about an order of magnitude at $\mathbf{p}_{\psi\rm T} > 3\,\mathrm{GeV}$ for $z \sim 0.8$. Also we note that in the region $z < 0.3$ the contribution of the resolved photon process may be large [47], as in the leptoproduction case.

The double differential cross sections $\mathrm{d}\sigma/\mathrm{d}\mathbf{p}^2_{\psi\rm T}\mathrm{d}z$ (Fig. 8) in the different z regions $0.3 < z < 0.6$ (Fig. 8a), $0.6 < z < 0.75$ (Fig. 8b) and $0.75 < z < 0.9$ (Fig. 8c) are well described by the $k_{\rm T}$-factorization approach.

It can be seen that the results obtained with the JB unintegrated gluon distribution with $\Delta = 0.35$ and the KMS ones (which effectively included the main part of the full NLO corrections to the value of Δ) practically coincide in a wide kinematical region, as in the leptoproduction case.

Figures 6–8 show that the $k_{\rm T}$-factorization results for inelastic J/ψ photoproduction with the realistic value of the charm mass $m_c = 1.55\,\mathrm{GeV}$ agree well with the H1 and ZEUS experimental data without any additional $c\bar{c} \to J/\psi$ fragmentation mechanisms, such as CO contributions.

3.3 Polarization properties of the J/ψ meson at HERA

As was mentioned above, one of the differences between the $k_{\rm T}$-factorization approach and the SPM is connected with the polarization properties of the final particles. In the present paper for studying the J/ψ meson polarization properties we calculate the $\mathbf{p}_{\rm T}$ and the z dependences of the spin alignment parameter α [14–16]:

$$\alpha(\omega) = \frac{\mathrm{d}\sigma/\mathrm{d}\omega - 3\mathrm{d}\sigma_{\rm L}/\mathrm{d}\omega}{\mathrm{d}\sigma/\mathrm{d}\omega + \mathrm{d}\sigma_{\rm L}/\mathrm{d}\omega}, \tag{19}$$

where $\sigma_{\rm L}$ is the production cross section for the longitudinally polarized J/ψ mesons, and $\omega = \mathbf{p}_{\psi\rm T}, z$. The parameter α controls the angular distribution for the leptons in the decay $J/\psi \to \mu^+\mu^-$ (in the J/ψ meson rest frame):

$$\frac{\mathrm{d}\Gamma(J/\psi \to \mu^+\mu^-)}{\mathrm{d}\cos\theta} \sim 1 + \alpha\cos^2\theta. \tag{20}$$

The cases $\alpha = 1$ and $\alpha = -1$ correspond to transverse and longitudinal polarizations of the J/ψ meson, respectively.

In our previous paper [16] we analyzed in detail the Q^2 and $\mathbf{p}^2_{\psi\rm T}$ dependences of the spin parameter α in the leptoproduction case. We found that it is impossible to make exact conclusions about the BFKL gluon contribution to the polarized J/ψ production cross section because of a large additional contribution from the initial longitudinal polarization of the virtual photons. However at low Q^2 and in the photoproduction limit these contributions are negligible. This fact should result in observable spin effects of

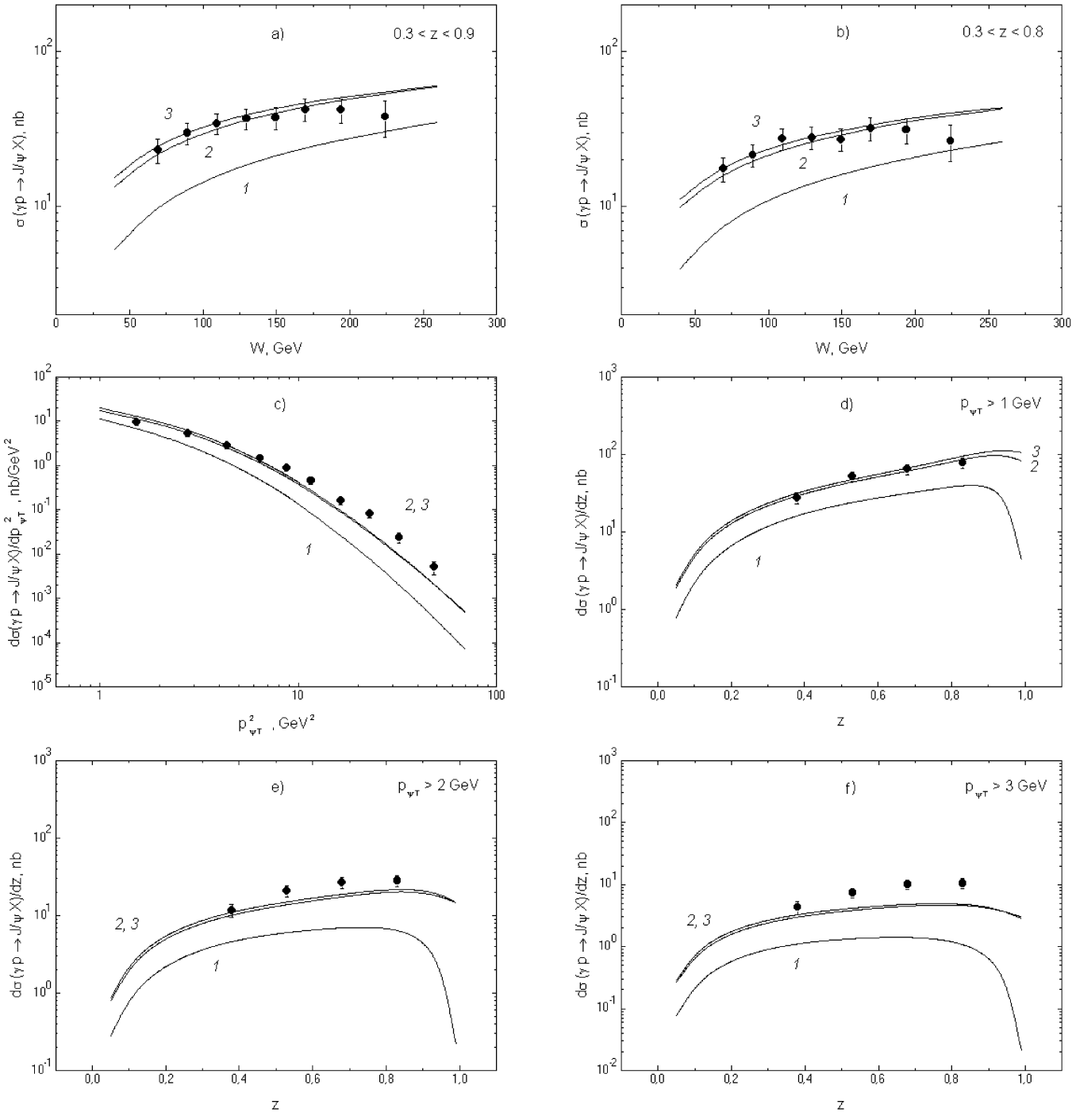

Fig. 6a–f. The total and single differential cross sections of the inelastic J/ψ photoproduction obtained in the kinematical region $60 < W < 240\,\text{GeV}$, $1 < p^2_{\psi\rm T} < 60\,\text{GeV}^2$, $0.3 < z < 0.9$ in comparison with the H1 [38] data. Curves 1–3 are the same as in Fig. 3

the final J/ψ mesons, connected with the $k_{\rm T}$-factorization effects. In this paper we have performed such calculations for the inelastic J/ψ photoproduction process.

The results of our calculations are shown in Figs. 9 and 10. Figure 9 shows the parameter α as a function z and $\mathbf{p}_{\psi\rm T}$ in comparison with the H1 experimental data which are obtained in the kinematical region $60 < W < 240\,\text{GeV}$, $0.3 < z < 0.9$ and $1 < \mathbf{p}^2_{\psi\rm T} < 60\,\text{GeV}^2$. Curve 1 corresponds to the SPM calculations in the leading order approximation with the GRV (LO) gluon density, curve 2 corresponds to the $k_{\rm T}$-factorization results obtained with the JB (at $\Delta = 0.35$ [17,23]) unintegrated gluon distribution. One can see that the z dependence of the spin parameter α is not sensitive to the results of different ap-

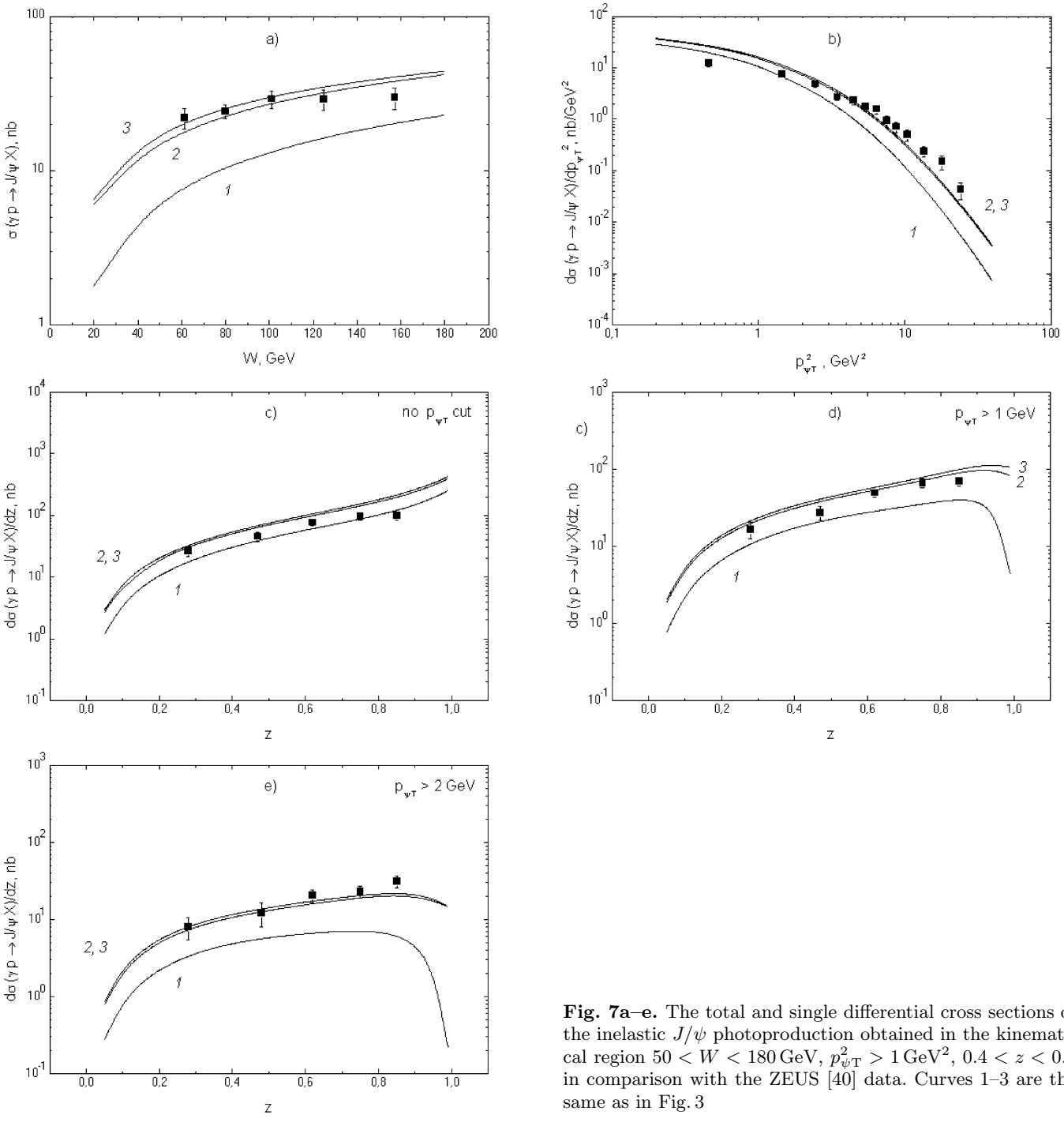

Fig. 7a–e. The total and single differential cross sections of the inelastic J/ψ photoproduction obtained in the kinematical region $50 < W < 180\,\text{GeV}$, $p^2_{\psi\rm T} > 1\,\text{GeV}^2$, $0.4 < z < 0.9$ in comparison with the ZEUS [40] data. Curves 1–3 are the same as in Fig. 3

proaches, including the non-relativistic QCD predictions (see [38]). However, the behavior of $\alpha(\mathbf{p}_{\rm T})$ is different in the $k_{\rm T}$-factorization approach and the SPM (see Fig. 9b). Although the experimental points have large errors they tend to support the $k_{\rm T}$-factorization theoretical predictions.

Figure 10 shows the $\mathbf{p}_{\psi\rm T}$ dependence of the spin parameter α in comparison with the ZEUS experimental data which are obtained in the kinematical region $50 < W < 180\,\text{GeV}$, $0.4 < z < 0.9$ (Fig. 10a,c) and $0.4 < z < 1$ (Fig. 10b,d). We note that in Fig. 10a,b the quantization axis is chosen to be opposite of the incoming proton direction in the J/ψ rest frame, θ is the opening angle between the quantization axis and the μ^+ direction of flight in the J/ψ rest frame. This frame is known as the "target frame" [40]. In Fig. 10c,d, the quantization axis was defined as the J/ψ direction of flight in the ZEUS coordinate system. This frame is known as the "helicity basis" [40,48]. Curves 1 and 2 are the same as in Fig. 9.

It is visible that only the $k_{\rm T}$-factorization approach gives a correct description of the ZEUS data, although the experimental points have large errors. We also have

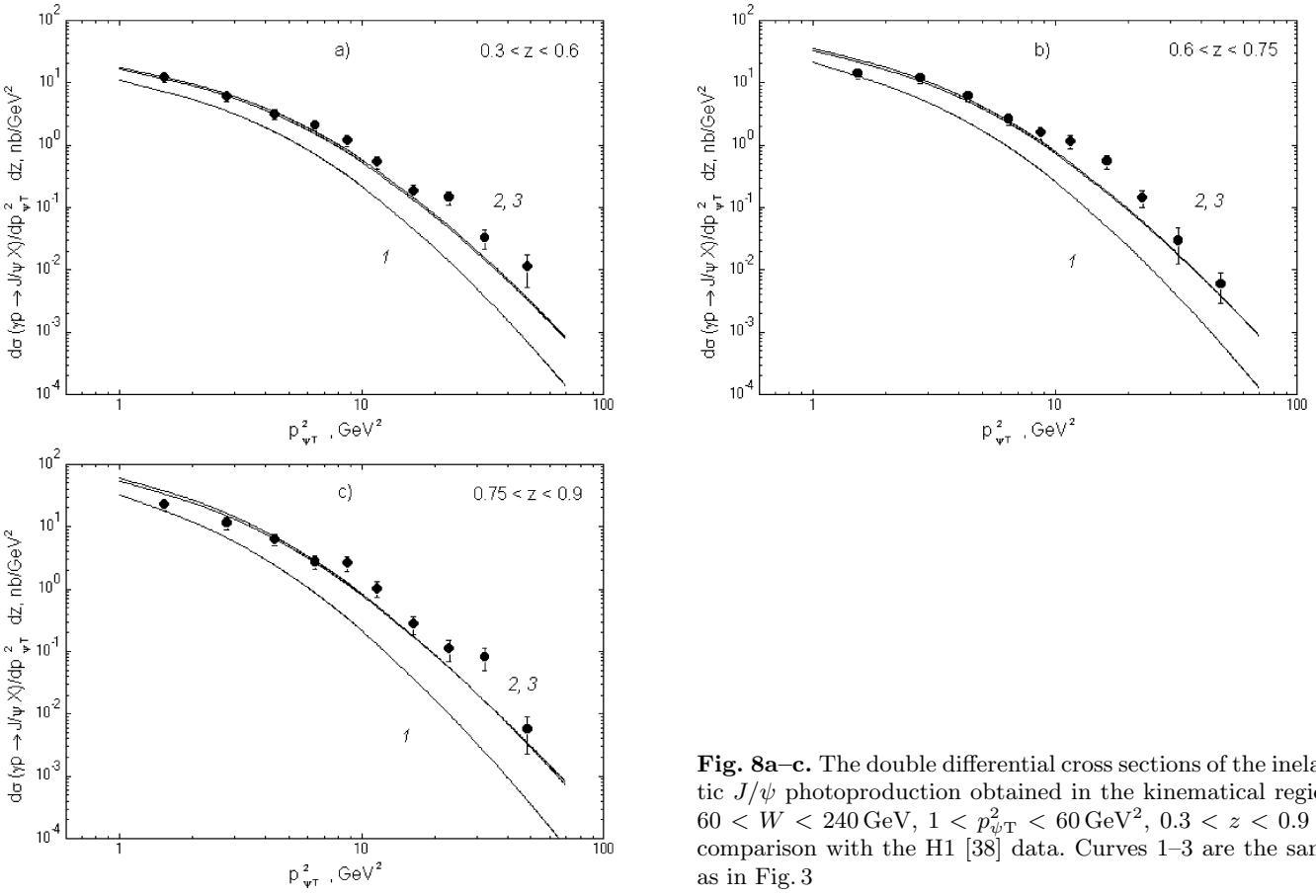

Fig. 8a–c. The double differential cross sections of the inelastic J/ψ photoproduction obtained in the kinematical region $60 < W < 240\,\text{GeV}$, $1 < p^2_{\psi\rm T} < 60\,\text{GeV}^2$, $0.3 < z < 0.9$ in comparison with the H1 [38] data. Curves 1–3 are the same as in Fig. 3

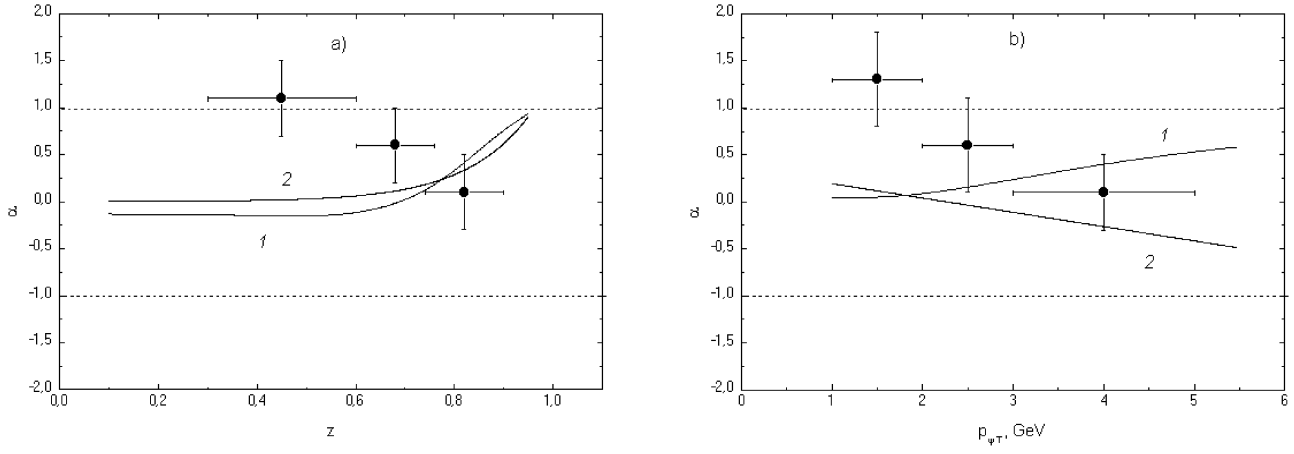

Fig. 9a,b. The parameter α as a function z and $p_{\psi\rm T}$ for the inelastic J/ψ photoproduction process which were obtained in the kinematical region $60 < W < 240\,\text{GeV}$, $0.3 < z < 0.9$ and $1 < p^2_{\psi\rm T} < 60\,\text{GeV}^2$ in comparison with the H1 [38] data. Curve 1 corresponds to the SPM calculations at the leading order approximation with the GRV (LO) gluon density, curve 2 corresponds to the $k_{\rm T}$-factorization QCD calculations with JB the unintegrated gluon distribution

a large difference between predictions of the leading order of SPM and the $k_{\rm T}$-factorization approach. The SPM predictions lie somewhat below the data at low $\mathbf{p}_{\psi\rm T}$ and somewhat above the data at high $\mathbf{p}_{\psi\rm T}$. Therefore the experimental measurement of the polarization properties of the J/ψ mesons will be an additional test of BFKL gluon dynamics.

4 Conclusions

In this paper we considered the inelastic J/ψ meson photo- and leptoproduction at HERA in the color singlet model using the standard parton model in leading order in $\alpha_{\rm S}$ and the $k_{\rm T}$-factorization QCD approach. We investigated the total cross section, the single differential and the dou-

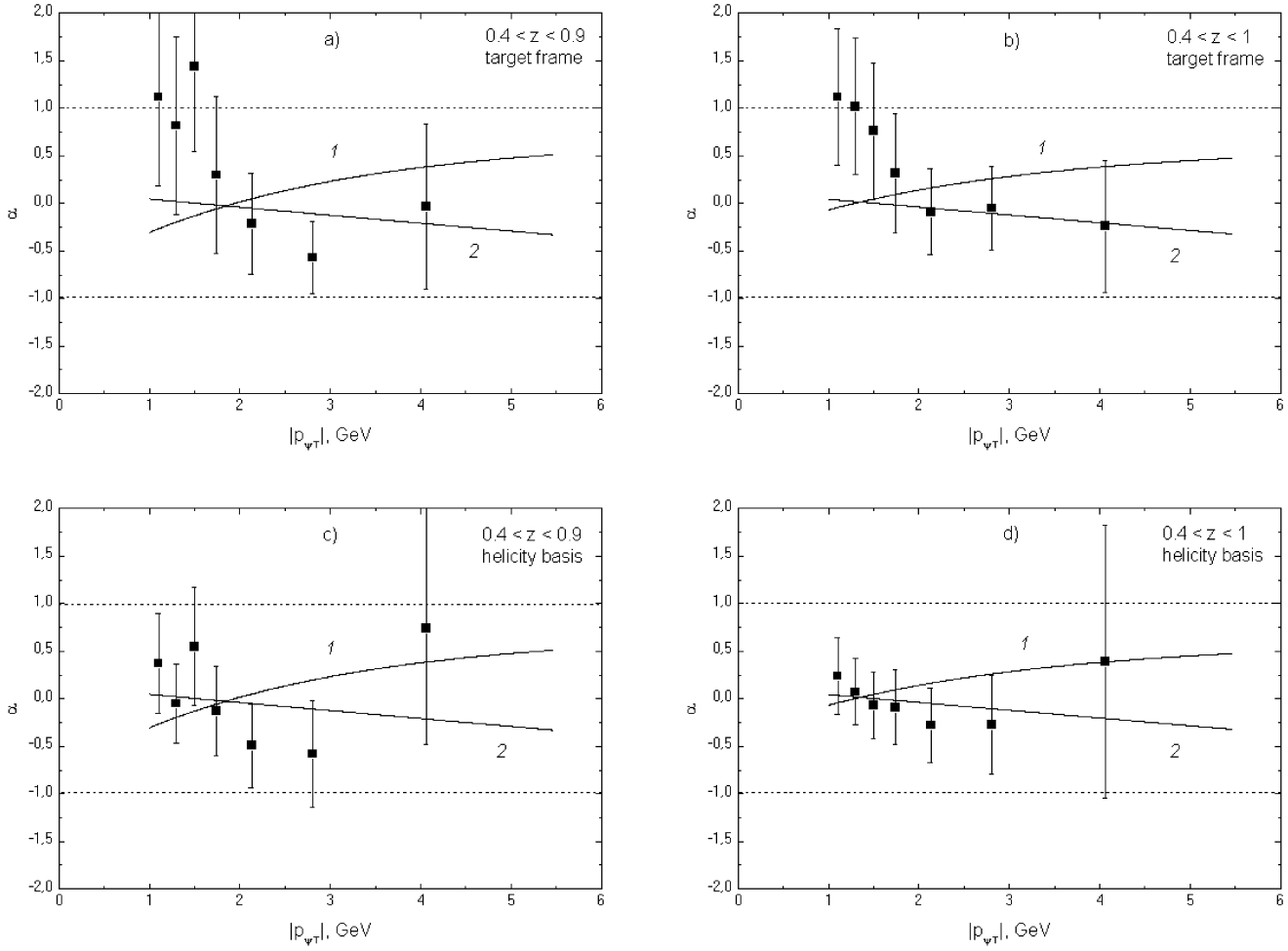

Fig. 10a–d. The parameter α as a function $p_{\psi \rm T}$ for the inelastic J/ψ photoproduction process which was obtained in the kinematical region $50 < W < 180\,\text{GeV}$, $0.4 < z < 0.9$ (Fig. 10a, c), $0.4 < z < 1$ (Fig. 10b, d) and $1 < p^2_{\psi \rm T} < 60\,\text{GeV}^2$ in comparison with the ZEUS [40] data. Curves 1 and 2 are the same as in Fig. 9

ble differential cross sections of inelastic J/ψ production on various forms of the unintegrated gluon distribution. The $\mathbf{p}_{\rm T}$ and z dependences of the spin alignment parameter α were also presented. We compared the theoretical results with recent experimental data taken by the H1 and ZEUS collaboration at HERA. We have found that the $k_{\rm T}$-factorization results (in contrast with the SPM ones) with the JB and KMS unintegrated gluon distributions agree well with the experimental data at the realistic value of the charm mass $m_c = 1.55\,\text{GeV}$, $|\psi(0)|^2 = 0.0876\,\text{GeV}^3$ and $\Lambda_{\rm QCD} = 250\,\text{MeV}$, without any additional transition mechanism from the $c\bar{c}$-pair to the J/ψ mesons (such as given by the CO model). We also found that the results obtained with the JB unintegrated gluon density at $\Delta = 0.35$ and the KMS one, which effectively included about 70% of the full NLO corrections to the pomeron intercept Δ, practically coincide in a wide kinematical region for J/ψ production processes at HERA conditions. Finally, it is shown that the experimental study of the polarization of the J/ψ meson at low $Q^2 < 1\,\text{GeV}^2$ should be an additional test of BFKL gluon dynamics.

Acknowledgements. The authors would like to thank S. Baranov for encouraging interest and useful discussions. A.L. thanks also V. Saleev for the help on the initial stage of work. The study was supported in part by RFBR grant 02-02-17513 and INTAS grant YS 2002 N399.

References

1. E. Berger, D. Jones, Phys. Rev. D **23**, 1521 (1981); S. Gershtein, A. Likhoded, S. Slabospitsky, Sov. J. Nucl. Phys. **34**, 128 (1981); R. Baier, R. Ruckl, Nucl. Phys. B **218**, 289 (1983)
2. L. Gribov, E. Levin, M. Ryskin, Phys. Rep. **100**, 1 (1983)
3. S. Catani, M. Ciafoloni, F. Hautmann, Nucl. Phys. B **366**, 135 (1991)
4. J. Collins, R. Ellis, Nucl. Phys. B **360**, 3 (1991)
5. E. Levin, M. Ryskin, Yu. Shabelsky, A. Shuvaev, Yad. Fiz. **53**, 1059 (1991)
6. E. Kuraev, L. Lipatov, V. Fadin, Sov. Phys. JETP **44**, 443 (1976); **45**, 199 (1977); Yu. Balitsky, L. Lipatov, Sov. J. Nucl. Phys. **28**, 822 (1978)

7. B. Andersson et al. (The Small x Collab.), Eur. Phys. J. C **25**, 77 (2002); hep-ph/0204115
8. M. Ryskin, Yu. Shabelski, Z. Phys. C **69**, 269 (1996)
9. M. Ryskin, Yu. Shabelski, A. Shuvaev, Phys. Atom. Nucl. **64**, 1995 (2001); Yad. Fiz. **64**, 2080 (2001)
10. V. Saleev, N. Zotov, Mod. Phys. Lett. A **9**, 151 (1994)
11. V. Saleev, N. Zotov, Mod. Phys. Lett. A **11**, 25 (1996)
12. A. Lipatov, N. Zotov, Mod. Phys. Lett. A **15**, 695 (2000)
13. A. Lipatov, V. Saleev, N. Zotov, Mod. Phys. Lett. A **15**, 1727 (2000)
14. S. Baranov, A. Lipatov, N. Zotov, in Proceedings of the 9th International Workshop on DIS and QCD (DIS'2001), Bologna, Italy, 2001, hep-ph/0106229
15. S. Baranov, Phys. Lett. B **428**, 377 (1998)
16. A. Lipatov, N. Zotov, hep-ph/0208237; to be published in Yad. Fiz. (2003)
17. S. Baranov, N. Zotov, Phys. Lett. B **458**, 389 (1999); B **491**, 111 (2000)
18. S. Baranov, M. Smizanska, Phys. Rev. D **62**, 014012 (2000)
19. P. Hagler, R. Kirschner, A. Schefer et al., Phys. Rev. D **62**, 071502 (2000)
20. H. Jung, Phys. Rev. D **65**, 034015 (2002); hep-ph/0110034
21. P. Hagler, R. Kirschner, A. Schefer et al., Phys. Rev. D **63**, 077501 (2001); F. Yuan, K.-T. Chao, Phys. Rev. D **63**, 034006 (2001); Phys. Rev. Lett. **87**, 022002 (2001), hep-ph/0009224
22. H. Jung, in Proceedings of Photon'2001, Ascona, Switzerland, hep-ph/0110345
23. S. Baranov, H. Jung, L. Jonsson et al., Eur. Phys. J. C **24**, 425 (2002); hep-ph/0203025
24. E. Braaten, S. Fleming, Phys. Rev. Lett. **74**, 3327 (1995); E. Braaten, T. Yuan, Phys. Rev. D **52**, 6627 (1995)
25. P. Cho, A. Leibovich, Phys. Rev. D **53**, 150 (1996); D **53**, 6203 (1996)
26. G. Bodwin, E. Braaten, G. Lepage, Phys. Rev. D **51**, 1125 (1995); D **55**, 5853 (1997)
27. M. Cacciari, M. Kramer, Phys. Rev. Lett. **76**, 4128 (1996)
28. P. Ko, J. Lee, H. Song, Phys. Rev. D **54**, 4312 (1996); D **60**, 119902 (1999)
29. S. Aid et al. (H1 Collab.), Nucl. Phys. B **472**, 3 (1996)
30. J. Breitweg et al. (ZEUS Collab.), Z. Phys. C **96**, 599 (1997)
31. S. Fleming, T. Mehen, Phys. Rev. D **57**, 1846 (1998)
32. B. Kniehl, L. Zwirner, Nucl. Phys. B **621**, 337 (2002); hep-ph/0112199
33. C. Adloff et al. (H1 Collab.), DESY-99-026
34. J. Korner, J. Cleymans, M. Kuroda, G. Gounaris, Phys. Lett. B **114**, 195 (1982)
35. J.-Ph. Guillet, Z. Phys. C **39**, 75 (1988)
36. H. Merabet, J. Mathiot, R. Mendez-Galain, Z. Phys. C **62**, 639 (1994)
37. F. Yuan, K.-T. Chao, Phys. Rev. D **63**, 034017 (2001)
38. C. Adloff et al. (H1 Collab.), Eur. Phys. J. C **25**, **1**, 25 (2002)
39. C. Adloff et al. (H1 Collab.), Eur. Phys. J. C **25**, **1**, 41 (2002)
40. S. Chekanov et al. (ZEUS Collab.), DESY 02-163
41. M. Beneke, M. Kramer, Phys. Rev. D **55**, 5269 (1997)
42. J. Blumlein, DESY 95-121
43. J. Kwiecinski, A. Martin, A. Stasto, Phys. Rev. D **56**, 3991 (1997)
44. M. Kramer, Nucl. Phys. B **459**, 3 (1996)
45. P. Ball, M. Beneke, V. Braun, Phys. Rev. D **52**, 3929 (1995)
46. E. Levin, M. Ryskin, Yu. Shabelsky, A. Shuvaev, Yad. Fiz. **54**, 1420 (1991)
47. H. Jung, G. Schuler, J. Terron, DESY-92-028
48. T. Affolder et al. (CDF Collab.), Phys. Rev. Lett. **85**, 2886 (2000)